Stroboscopic fluorescence lifetime imaging

Mark D. Holton,[1] Oscar R. Silvestre,[2] Rachel J. Errington,[2] Paul J. Smith,[2] Daniel R. Matthews,[3] Paul Rees[4] and Huw D. Summers.[4,*]

[1]*School of Medicine, Swansea University, Singleton Park, Swansea, SA2 8PP, U.K.*
[2]*School of Medicine, Cardiff University, Heath Park, Cardiff, CF14 4XN, U.K.*
[3]*Randall Division, Guy's Medical School Campus, King's College London,SE1 9RT, U.K.*
[4]*Multidisciplinary Nanotechnology Centre, School of Engineering, Swansea University, Swansea, SA2 8PP, U.K.*
[*]*Corresponding author: H.D.Summers@swansea.ac.uk*

Abstract: We report a fluorescence lifetime imaging technique that uses the time integrated response to a periodic optical excitation, eliminating the need for time resolution in detection. A Dirac pulse train of variable period is used to probe the frequency response of the total fluorescence per pulse leading to a frequency roll-off that is dependent on the relaxation rate of the fluorophores. The technique is validated by demonstrating wide-field, real-time, lifetime imaging of the endocytosis of inorganic quantum dots by a cancer cell line. Surface charging of the dots in the intra-cellular environment produces a switch in the fluorescence lifetime from ~ 40 ns to < 10 ns. A temporal resolution of half the excitation period is possible which in this instance is 15 ns. This stroboscopic technique offers lifetime based imaging at video rates with standard CCD cameras and has application in probing millisecond cell dynamics and in high throughput imaging assays.

OCIS codes: (170.0170) Microscopy; (170.6920) Time-resolved imaging; (120.3890) Medical optics instrumentation; (170.1530) Cell analysis; (170.2520) Fluorescence microscopy.

References and links

1. F. S. Wouters, P. J. Verveer, and P. I. Bastiaens, "Imaging biochemistry inside cells," Trends Cell Biol. **11**, 203-211 (2001).
2. K. Suhling, P. M. W. French, and D. Phillips, "Time resolved fluorescence microscopy," Photochem. Photobiol. Sci. **4**, 13–22 (2005).
3. R. Cubeddu, P. Taroni, and G. Valentini, "Time-gated imaging system for tumor diagnosis," Opt. Eng. **32,** 320-324 (1993).
4. C. G. Morgan, A. C. Mitchell, and J. G. Murray, "Nanosecond Time-Resolved Fluorescence Microscopy: Principles and Practice," Proc.R. Microsc. Soc. **1**, 463–466 (1990).
5. E. P. Buurman, P. Sanders, A. Draaijer, H. C. Gertitsen, J. J. F. van Veen, P. M. Houtpt, and Y. K. Levine, "Fluorescence lifetime imaging using a confocal laser scanning microscope," Scanning **14**, 155–159 (1992).
6. I. Bugiel, K. Konig, and H. Wabnitz, "Investigation of cells by fluorescence laser scanning microscopy with subnanosecond time resolution," Lasers Life Sci. **3**, 47–53 (1989).
7. X. F. Wang, T. Uchida, D. M. Coleman, and S. Minami, "A 2-dimensional fluorescence lifetime imaging-system using a gated image intensifier," Appl Spectrosc. **45**, 360–366 (1991).
8. K. Dowling, M. J. Dayel, M. J. Lever, P. M. W. French, J. D. Hares, and A. K. L. Dymoke-Bradshaw, "Fluorescence lifetime imaging with picosecond resolution for biomedical applications," Opt. Lett. **23**, 810-812 (1998).
9. J. R. Lakowicz, H. Szmacinskia, K. Nowaczyka, K. W. Berndta, and M. Johnson, "Fluorescence lifetime imaging," Anal. Biochem. **202**, 316-330 (1992).
10. R. M. Clegg, G. Marriott, B. A Feddersen, E. Gratton, and T. M. Jovin, "Sensitive and rapid determinations of fluorescence lifetimes in the frequency domain in a light-microscope," Biophys. J. **57,** A375–A375 (1990).
11. D. R. Matthews, H. D. Summers, K. Njoh, R. J. Errington, P. J. Smith, P. Barber, S. Ameer-Beg, and B. Vojnovic, "Technique for measurement of fluorescence lifetime by use of stroboscopic excitation and continuous-wave detection," Appl. Opt. **45**, 2115-2123 (2006).
12. Y. Sakai and S. Hirayama, "A fast deconvolution method to analyze fluorescence decays when the excitation pulse repetition period is less than the decay times," J. Lumin. **39**, 145-151 (1988).

#107281 - $15.00 USD Received 6 Feb 2009; revised 13 Mar 2009; accepted 15 Mar 2009; published 18 Mar 2009

13. M. Müller, R. Ghauharali, K. Visscher, and G. Brakenhoff, "Double-pulse fluorescence lifetime imaging in confocal microscopy," J. Microsc. **177**, 171-179 (1994).
14. H. Nyquist, "Certain topics in telegraph transmission theory," Trans. Am. Inst. Electr. Eng. **47**, 617-644 (1928).
15. T. Ng, A. Squire, G. Hansra, F. Bornancin, C. Prevostel, A. Hanby, W. Harris, D. Barnes, S. Schmidt, H. Mellor, P. I. H. Bastiaens, and P. J. Parker, "Imaging protein kinase Cα activation in cells," Science **283**, 2085-2089 (1999).
16. O. Holub, M. J. Seufferheld, C. Gohlke, Govindjee, and R. M. Clegg, "Fluorescence lifetime imaging (FLI) in real time – a new technique in photosynthesis research," Photosynthetica **38**, 581-599 (2000).
17. A. V. Agronskaia, L. Tertoolen, and H. C. Gerritsen, "High frame rate fluorescence lifetime imaging," J. Phys. D 36, 1655-1662 (2003).
18. D. J. Stephens and V. J. Allan, "Light microscopy techniques for live cell imaging," Science **300**, 82-86 (2003).
19. B. Dubertret, P. Skourides, D. J. Norris, V. Noireaux, A. H. Brivanlou, and A. Libchaber, "In vivo imaging of quantum dots encapsulated in phospholipid micelles," Science **298**, 1759-1762 (2002).
20. J. K. Jaiswal, H. Mattoussi, J. M. Mauro, and S. M. Simon, "Long-term multiple color imaging of live cells using quantum dot bioconjugates," Nature Biotech. **21**, 47-51 (2002).
21. A. Hoshino, K. Hanaki, K. Suzuki, and K. Yamamoto, "Applications of T-lymphoma labelled with fluorescent quantum dots to cell tracing markers in mouse body," Biochem. and Biophys. Res. Commun. **314**, 46-53 (2003).
22. Y. S. Liu, Y. H. Sun, P. T. Vernier, C. H. Liang, S. Y. C. Chong, and M. A. Gundersen, "pH-sensitive photoluminescence of CdSe/ZnSe/ZnS quantum dots in human ovarian cancer cells," J. Phys. Chem. **111**, 2872-2878 (2007).
23. Y. H. Sun, Y. S. Liu, P. T. Vernier, C. H. Liang, S. Y. Chong, L. Marcu, and M. A. Gundersen, "Photostability and pH sensitivity of CdSe/ZnSe/ZnS quantum dots in living cells," Nanotechnology **17**, 4469-4476 (2006).
24. S. J. Clarke, C. A. Hollmann, Z. Zhang, D. Suffern, S. E. Bradforth, N. M. Dimitrijevic, W. G. Minarik, and J. L. Nadeau, "Photophysics of dopamine-modified quantum dots and effects on biological systems," Nature Materials **5**, 409-417 (2006).
25. S. R. Cordero, P. J. Carson, R. A. Estabrook, G. F. Strouse, and S. K. Buratto, "Photo-activated luminescence of CdSe Quantum dot monolayers," J. Phys. Chem. **104**, 12137-12142 (2000).
26. N. E. Korunska, M. Dybiec, L. Zhukov, S. Ostapenko, and T. Zhukov, "Reversible and non-reversible photo-enhanced luminescence in CdSe/ZnS quantum dots," Semicond. Sci. Technol. **20**, 876-881 (2005).
27. M. Nirmal, B. O. Dabbousi, M. G. Bawendi, J. J. Macklin, J. K. Trautman, T. D. Harris, and L. E. Brus, "Fluorescence intermittency in single cadmium selenide nanocrystals," Nature **383**, 802-804 (1996).
28. C. D. McGuinness, K. Sagoo, D. McLoskey, and D. J. S. Birch, "A new sub-nanosecond LED at 280nm: application to protein fluorescence," Meas. Sci. Technol. **15**, L19-L22 (2004).

1. Introduction

Fluorescence imaging of biological material at tissue and single cell level is one of the most widely used techniques in biomedical science [1]. The use of fluorescence lifetime imaging (FLIM) has become particularly important because contrast based on a fluorescence decay rate rather than absolute intensity avoids signal variation due to effects such as inhomogeneous labelling, fluorophore diffusion or quenching and provides differentiation of tissue auto-fluorescence [2]. Spatial analysis of biological processes can also be achieved with a wide range of functional lifetime-based probes that report on key chemical markers such as oxygen, calcium or pH. FLIM may be implemented using either a time or frequency based measurement. In the time domain an ultra-short laser pulse provides impulse excitation followed by temporal resolution of the detected fluorescence [3,4]. This can be implemented with a single channel detector using scanning microscopy [5,6] or in wide-field using multiple channel detectors such as gated CCD cameras [7,8]. In the frequency domain the lifetime is extracted from analysis of the phase shift and demodulation of the fluorescence with respect to a modulated excitation [9,10]. In all of the current FLIM techniques there is a requirement for temporal resolution and synchronisation of excitation and detection signals. We report a new approach that uses what is in effect a Dirac pulse train for excitation and derives lifetime based image contrast using time-integrated fluorescence. This 'stroboscopic' technique therefore completely removes the need for time resolved detection or synchronisation making FLIM faster, cheaper and easier to implement on existing fluorescence microscopes. We have

#107281 - $15.00 USD Received 6 Feb 2009; revised 13 Mar 2009; accepted 15 Mar 2009; published 18 Mar 2009

previously demonstrated the use of stroboscopic excitation to determine fluorescence lifetime in a non-imaging mode and explored the resolution and sensitivity of the technique [11].

The extraction of lifetime-based contrast for strobe-FLIM is based on the interaction of fluorophores with a periodic train of optical impulse excitations. In the case where the impulse frequency is greater than the fluorescence relaxation rate, the time-integrated response of the system becomes dependent upon the relaxation process. A short excitation repetition time such as this is normally avoided as it leads to incomplete recovery of the system [12]. Here we deliberately use the limited time cycle to inhibit fluorescence decay and so maintain a finite, minimum excited state population of fluorophores. This leads to a decrease in the absorption of the excitation signal and a non-linear fluorescence response to increasing excitation frequency: the time-integrated fluorescence is described by the exponential of the ratio of fluorescence decay rate to excitation pulse frequency. The system establishes a dynamic equilibrium in which each pulse cycle is identical and a balance is maintained between the energy transferred from the impulse and the energy released by fluorescence decay. Reducing the impulse period lowers the amount of energy absorbed during the cycle and therefore reduces the integrated response signal per impulse excitation. The schematic in Fig. 1 shows the time and frequency domain functions for strobe-FLIM analysis of a fluorophore with a single exponential decay rate, γ.

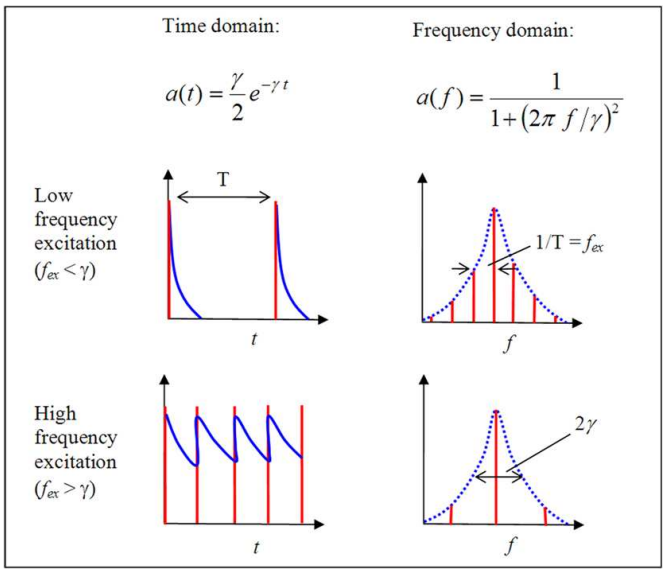

Fig. 1. Schematic of the stroboscopic excitation technique in time and frequency domains.

In the frequency domain the lifetime analysis may be viewed as a form of Fourier synthesis in which the temporal response of the system is reproduced by the frequency sampling imposed by the measurement. The impulse train maintains its waveform under Fourier transformation with the period, T and frequency spacing, f_{ex} of the pulse train being inversely proportional thus in strobe-FLIM the system is sampled by a multiple set of discrete frequencies and its response is dictated by the relative values of γ and f_{ex} (see equation 1). When the excitation period is very much greater than the fluorescence lifetime ($f_{ex} << \gamma$) the frequency sampling becomes quasi-continuous and a near-true representation of the decay waveform is achieved. This equates to repetitive time-domain lifetime measurement and produces a fluorescence pulse train that is linearly proportional to the excitation frequency and hence integrated fluorescence, Sc is independent of f_{ex}. Towards the high frequency limit for excitation ($f_{ex} \geq \gamma$) the pulse train resembles the frequency domain technique in that the temporal excitation signal Fourier transforms to a dc plus single frequency component and

#107281 - $15.00 USD Received 6 Feb 2009; revised 13 Mar 2009; accepted 15 Mar 2009; published 18 Mar 2009

produces a corresponding sinusoidal component within the time domain system response. The limited sampling produces a constant dc background with associated absorption saturation which leads to a frequency dependent Sc. Thus the stroboscopic technique sits between the time and frequency domain methods using a frequency-swept, periodic impulse excitation which equates to the traditional analyses in the limit, and in bridging them provides the unique capability of time resolution with time integrated detection.

A rate equation based analysis of these temporal dynamics can be used to obtain an analytical description of the total fluorescence per excitation cycle:

$$S_c = \kappa \left[\frac{e^{2\alpha P} - 1}{e^{2\alpha P} - e^{-\frac{\gamma}{f_{ex}}}} \right] \left(1 - e^{-\frac{\gamma}{f_{ex}}} \right) \quad (1)$$

where γ and f_{ex} are the fluorescence relaxation rate and excitation frequency respectively, P is the number of excitation events per impulse, κ is a collection efficiency and α an excitation efficiency. The term in square brackets in equation 1 is a ratio of the number of excitation events per pulse and the maximum number of excitation events possible for all fluorophores in the ground state i.e. it represents an excitation efficiency determined by the constant presence of excited state fluorophores. The second bracketed term describes the reduction in total fluorescence due to the incomplete decay. A theoretical analysis of the measurement of fluorescence lifetime via the time integrated signal has been presented previously based on the use of a double-pulse excitation [13]. In this case because only two pulses are used the system must be excited to transparency to ensure an equal excited state population immediately following each of the impulses or alternatively corrections made to account for the non steady-state excitation. By introducing a periodic impulse train we allow the system to reach a cyclic equilibrium in which each impulse response is identical through natural evolution of the fluorescence excitation and decay dynamics. This essentially allows us to implement the technique using excitation powers well below (< 10%) what is required to produce fluorescence saturation [11].

2. Results

2.1 Frequency response of integrated fluorescence

An example of time inhibited fluorescence decay in response to a periodic impulse excitation is shown in Fig. 2(a). The fluorescence emission from 705 nm wavelength, CdTe / ZnS quantum dots (QDs) in aqueous solution is time resolved using a streak camera detector over a range of excitation frequencies. The impulse train is provided by a picosecond pulse, from a white-light laser via a 600 nm short pass filter (Fig. 2(a).). The response at 1 MHz shows complete inter-pulse recovery of the fluorescence and a single exponential fit to the data (Fig. 2(b).) indicates a QD relaxation rate, γ = 23 ± 2 MHz (τ = 43 ± 4 ns). A simple, single component fit is adopted as this equates to the stroboscopic methodology. Due the limited relaxation rate at the higher excitation frequencies (f_{ex} > 10 MHz) there is incomplete relaxation to the ground state. In this example the peak fluorescence intensity is independent of frequency indicating excitation to saturation. A fit to the frequency roll-off in the total fluorescence per pulse (Fig. 2(c).), using equation 1 in the high excitation limit ($e^{2\alpha P} >> 1$), gives a value of γ = 21 ± 4 MHz, in good agreement with the directly time-resolved value. The accuracy of the γ measurement is determined by the relative range of the frequency sweep and the level of intensity noise in the fluorescence signal. Because the frequency roll-off can be described in terms of frequency sampling, a frequency domain formulation of the familiar Nyquist sampling theorem [14] can be adopted to assess the measurement maximum, γ_{max} (minimum τ). Incomplete sampling arises when giving $\gamma_{max} = 2f_{max}$., which for this work equates to 60 MHz (f_{max} = 30 MHz).

#107281 - $15.00 USD Received 6 Feb 2009; revised 13 Mar 2009; accepted 15 Mar 2009; published 18 Mar 2009

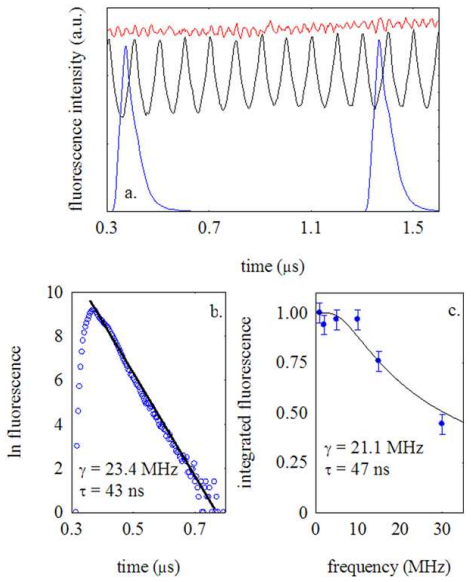

Fig. 2. (a) Streak camera data for excitation frequencies of 1 MHz (blue trace), 10 MHz (black trace) and 30 MHz (red trace) illustrating the inhibited fluorescence decay of 705 nm quantum dots in response to a periodic impulse; (b) a single-exponential fit to the complete inter-pulse recovery of the 705 nm quantum dots under 1 MHz excitation and (c) the frequency roll-off of integrated fluorescence per pulse as the inter-pulse period is reduced to less than the quantum dot lifetime. The solid line is a best-fit to the data using equation 1, the parameter values of which are shown.

2.2 Fluorescence lifetime imaging

The experimental setup for implementation of the stroboscopic technique for lifetime imaging is shown in Fig. 3(a). The pulsed laser is directly coupled to a fluorescence microscope via the lamp port and wide-field images are collected via a 40x, 0.75 N.A. lens using a 20 ms exposure time. The beam passes through spectral filters to remove the red and infra-red part of the spectrum and a focusing lens that is adjusted to achieve full illumination of the image field. The excitation power density within the central, 50x50 μm area of the image is 500 W cm^{-2} . In this mode we adopt a ratio metric measure (a 'frequency ratio') for image contrast of $R = \frac{30\, I_{1MHz}}{I_{30MHz}}$ where I is the image intensity, for a fixed exposure time, at the appropriate excitation frequency. We then define a characteristic frequency of the system, f_0 using the measured response at 30 MHz: $f_0 = 30 \ln\left[\frac{R}{(R-1)}\right]$. This empirical approach provides a measure of the frequency response of the system and avoids inappropriate identification of a fluorescence 'lifetime' with the associated assumption of a single, exponential decay. Whilst f_0 does not directly equate to γ it does provide a quantitative assessment of the dynamics of the fluorescence response. Thus the important point in relation to practical lifetime microscopy is that the frequency ratio, R will correlate with the fluorescence decay and so provides image contrast related to the lifetime rather than intensity of fluorescence. The frequency-ratio image requires measurement of just two images with ~ 20 ms exposure time and so lifetime based imaging can be achieved at video rates. The images in Fig. 3 show strobe-FLIM of inorganic (705 and 611 nm QDs) and organic (Cy-5) fluorophores deposited and dried onto glass cover slips to form touching boundaries between the two species. The fluorescence intensity and ratio images are shown in Fig. 3(b-e), there is a clear discrimination in the ratiometric images between the three fluorophores. The 611 nm QDs (CdSe/ZnS) have a 1/e lifetime of ~ 35 ns

#107281 - $15.00 USD Received 6 Feb 2009; revised 13 Mar 2009; accepted 15 Mar 2009; published 18 Mar 2009

(measured from time resolved, streak camera trace) leading to a mean R value ~ 2, the contrast of these with the longer lifetime 705 nm dots (CdTe/ZnS), with mean R ~ 3, can be clearly resolved. The origin of the large fractional range in R values for both QD types (~ 100% variation) is unclear but may be due to density fluctuations in the nanoparticle films. The decay rate of the Cy-5 is well in excess of the experimental range (~ 1 GHz) and so a linear frequency response with R ~ 1 is measured in this case.

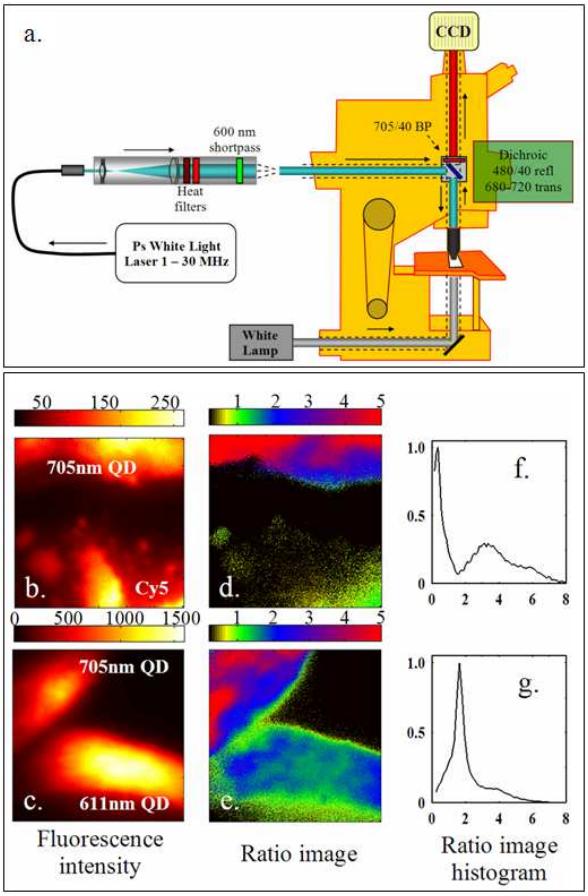

Fig. 3. (a) Experimental setup illustrating the laser input at the upper lamp input-port and the spectral filters used for imaging; (b) 50 x 50 μm, fluorescence intensity images of 705 nm QDs and Cy-5 dye and (c) 705 nm and 611 nm QDs; (d) ratio images derived from intensity images taken at 1 MHz and 30 MHz excitation frequencies for 705 nm QDs and Cy-5 and (e) 705 nm and 611 nm QDs; (f) histograms of pixel-to-pixel variation in R for 705 nm QDs and Cy-5 and (g) 705 nm and 611 nm QDs. In both cases the distribution is bi-modal illustrating the ability of stroboscopic imaging to distinguish the fluorophore pairs from their lifetime.

The maximum intensity variation in successive images is ± 5% (single pixel variation) and so the error margin in R is ± 7%. The characteristic frequencies for the 611 nm and 705 nm QDs are 29 ± 3 MHz and 12 ± 1 MHz respectively. A statistical analysis of the frequency ratio is also shown in Fig. 3(f-g). in the histograms of the pixel-to-pixel variation, each histogram represents data summed from three images. A bi-modal distribution is obtained in each case with the broader, 705 nm QD peak clearly discernible from the lower ratio 611 nm QD and Cy5 maxima.

#107281 - $15.00 USD Received 6 Feb 2009; revised 13 Mar 2009; accepted 15 Mar 2009; published 18 Mar 2009

2.3 Imaging fluorescence dynamics in living cells

FLIM has been successfully used for live cell imaging [15]. Whilst real-time, live-cell FLIM has been successfully demonstrated [16, 17] it is a challenging technique to apply to living cells as the potentially long exposure times associated with the determination of a decay time can lead to photo-damage [18]. The major advantage of the strobe-FLIM technique is its speed of image acquisition and so it is potentially much easier to apply to live cell applications. To validate this hypothesis we used it to image the endocytic uptake and processing of 705 nm wavelength, colloidal QDs by a human Osteosarcoma cell line (U-2 OS). Whilst QDs have been shown to be photo and bio-stable enough to be used as multi-generational (over 5 generations) fluorescent reporters [19, 20] there have been reports of a reduction in fluorescence efficiency when placed in cells [21] and their fluorescence lifetime has been shown to be sensitive to local pH [22, 23]. Indeed these nanoparticles have been conjugated to dopamine molecules and used as bio-sensors informing on intra-cellular redox potential via changes in the QD quantum yield [24].

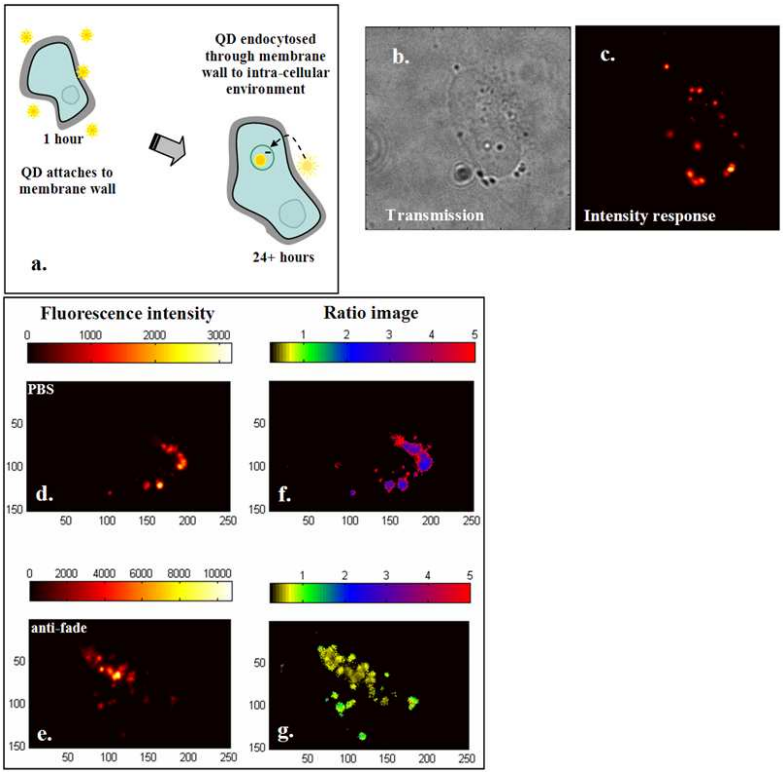

Fig. 4. (a) schematic of the QD uptake and localisation within intra-cellular vesicles via endocytosis; (b) typical 50 x 50 μm, transmission and (c) fluorescence intensity images of a single cell; (d) 50 x 30 μm intensity image of a cell, fixed in PBS 24 hours following QD uptake and (e) intensity image of a cell fixed in Prolong® Gold, anti-fade reagent 24 hours following QD uptake; (f) corresponding ratio images for cells fixed in PBS and (g) anti-fade reagent.

The fundamental process underlying these effects is charge transfer to and from surface states on the nanoparticle. When charge neutral the dots exist in a 'bright' state with high radiative efficiency, subsequent charge capture into surface traps leads to a 'dark' state in which rapid non-radiative relaxation is dominant [25, 26]. For individual dots this leads to a 'blinking' of the fluorescence as charge is transferred to and from the dot surface [27]. For QD ensembles the cumulative effect is a quantum yield and fluorescence lifetime that is

#107281 - $15.00 USD Received 6 Feb 2009; revised 13 Mar 2009; accepted 15 Mar 2009; published 18 Mar 2009

dependent upon the redox potential of the local environment. The uptake of QDs via endocytosis and their subsequent encapsulation within acidic organelles therefore provides an ideal system in which to look for fluorescence lifetime changes.

Our initial work adopted the approach of Sun et al. [23] and used fixed cells in different buffers to demonstrate the potential of strobe-FLIM to provide spatially resolved read-out of redox state. The delivery of the dots by endocytosis leads to their concentration within discrete sub-cellular compartments (fig. 4(a-c).). We image the QD fluorescence from cells that are fixed at 24 hours post loading, at this point in the endocytic cycle there is peri-nuclear, punctate localisation of the fluorescence from QDs within the endosomal compartments. The reduction potential of the intra-cellular medium is controlled by the introduction of an anti-fade reagent – Prolong® Gold (Invitrogen); this is designed to act as an anti-oxidant with the aim of reducing photo-bleaching of organic fluorophores. When used with QDs the opposite is achieved as chemical reduction by the anti-oxidant charges the dots and so reduces the quantum yield (QY) [24]. Images (50 x 30 micron field) of the QDs within fixed cells in phosphate buffered saline (PBS) or anti-fade solutions are shown in Fig. 4(d). and 4(e). The results for cells fixed in pH neutral, PBS buffer indicate R values ~ 2-3 (f_0 ~ 16 MHz) indicating that the lifetime of the dots is little altered by the process of cellular targeting and uptake. The ratio images of cells in anti-fade reagent show a linear, R response indicating a fluorescence lifetime below the system resolution of 15 ns as expected given the dominance of short lifetime, non-radiative relaxation within surface charged dots. Continuous monitoring of R as the anti-fade agent is added to a PBS buffered sample shows an immediate reduction in fluorescence intensity and a switch in R from 2-3 to 1. We are confident therefore that the low R values are due to the external agent rather than cellular processes. To corroborate these results the cells were also imaged using time domain FLIM within a scanning, time-correlated, single photon counting (TCSPC) system (Nikon microscope with Becker and Hickl acquisition system). Two-photon excitation at 850 nm wavelength was used with an average power of 800 mW and an image acquisition time 2 minutes. For the cells fixed in PBS there is a continuous base-level count and no reliable tau value can be obtained. We attribute this to fluorescence build-up from previous excitation periods due to QD lifetimes well in excess of the TCSPC repetition time of 12.5 ns. The TCSPC results for the cells fixed in anti-fade reagent indicate a decay lifetime of ~ 300 ps and so confirm that the observation of R = 1 with strobe-FLIM is due to lifetime reduction below the resolution of the measurement. These fixed-cell experiments establish that, within the 10-100 ns lifetime regime of QDs, strobe-FLIM is able to provide spatial resolution of fluorophore dynamics and in the example shown allows correlation of intensity changes within the cellular environment with QY changes and a corresponding reduction in fluorescence lifetime.

Imaging of live cells was done over 5 days, maintaining the U-2 OS cells at 36.5 ± 0.2^{o} C on a heated microscope stage within sealed chambers on a multi-well plate. The excitation power was once again 500 Wcm^{-2} and lifetime based ratio metric imaging was done at 4 frames per second (2 Hz ratio imaging) using 20 ms exposure times on a daily basis. Whilst a detailed analysis of the cell cycle dynamics under these conditions was not undertaken there was clear evidence of progression through mitosis and hence cell proliferation throughout the time period. Thus it was possible to undertake live cell FLIM without marked photo-induced cell perturbation and with minimal cell death.

#107281 - $15.00 USD Received 6 Feb 2009; revised 13 Mar 2009; accepted 15 Mar 2009; published 18 Mar 2009

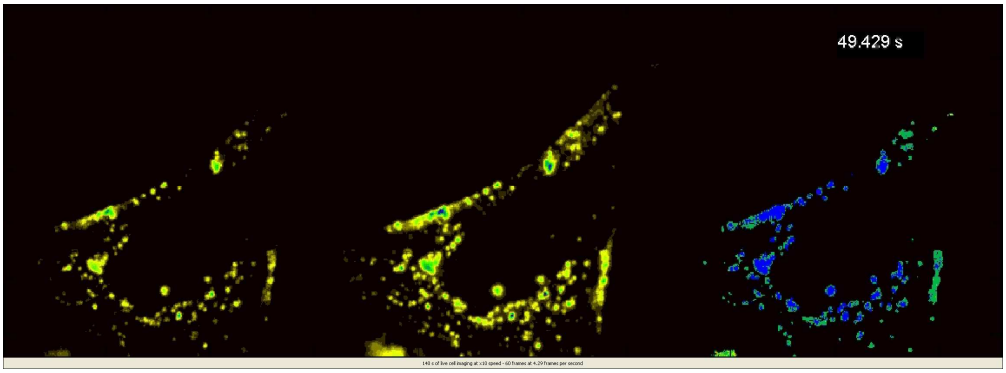

Fig. 5. (Media 1) shows 140 seconds of imaging time at x10 speed. From left to right, the first two images are the raw data taken at 1 MHz and 30 MHz repetition rates respectively and the final image is the frequency ratio, R. Rapid motion of the QD loaded vesicles can be seen and this temporal resolution is maintained in the ratio image.

A time-lapse movie covering 140 seconds of cell imaging using fluorescence intensity and intensity ratio, R is shown in Fig. 5. The imaging speed is sufficient to avoid blurring due to whole cell motion and is even quick enough to capture the rapid intra-cellular dynamics of endosome trafficking. The longer term dynamics are given in Fig. 6 where ratio metric images taken at 1, 2 and 5 days are shown in Fig. 6(a-c). together with histograms of the R values (fig. 6(d).). The histograms are averages of 4 cell images taken at each of the time points. There was minimal change in R during the process of QD internalisation, indeed the absolute fluorescence intensity and ratio metric measure was constant for the first 48 hours following QD loading. This is not surprising as the Qtracker® system used is designed to provide long term stability within live cells. Over the full 5 days however there was a clear reduction in fluorescence intensity and a corresponding change in R. This is presumably due to QD degradation with associated surface charging leading to an increased non-radiative decay rate and a concomitant reduction in quantum yield and fluorescence lifetime. After 100+ hours in the cell the QD fluorescence intensity is reduced to ~ 1/3 of its original value and the mean R value reduces from ~ 2.5 (f_0 ~ 15 MHz) to 1.9 (f_0 ~ 22 MHz).

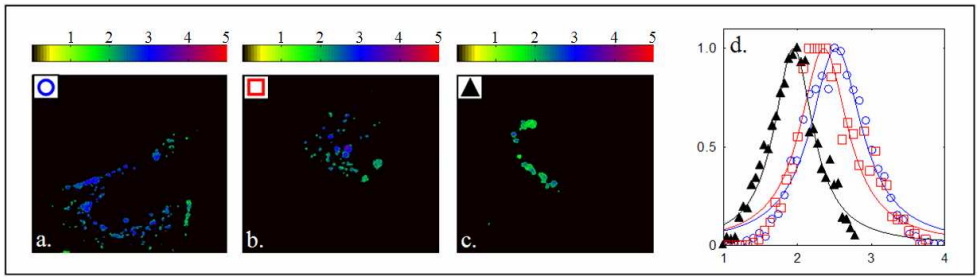

Fig. 6. (a) 30 x 30 µm, Ratio images of live cells at 24 hours post QD loading, (b) 48 hours post QD loading and (c) 120 hours post QD loading; (d) the histograms of the R variation, the symbols on the insets of fig. 6a-c relate each trace to the corresponding acquisition time. The three histograms show a systematic reduction as the QDs are degraded within the cells leading to a reduced QY and a shorter τ as non-radiative relaxation routes become active.

3. Discussion

The novelty of strobe-FLIM is its ability to provide temporal analysis using time integrated fluorescence; this removes the need for specialist detectors making it straightforward and relatively cheap to install; future development could see the implementation of relatively inexpensive, mass manufactured, LED light sources [28] for excitation making it truly low-cost. Implementing lifetime measurement using only excitation control also removes any

#107281 - $15.00 USD Received 6 Feb 2009; revised 13 Mar 2009; accepted 15 Mar 2009; published 18 Mar 2009

requirement for synchronisation of excitation and detection signals and so strobe-FLIM is also easy to implement requiring only standard, wide-field fluorescence images from a CCD camera. The method cannot provide a complete description of the fluorescence decay relying rather on empirical measures that parameterise the fluorescence dynamics. The temporal resolution obtained is determined by the laser pulse frequency; and whilst this may be higher than reported here e.g. 1 GHz mode-locked Nd:YAG lasers are available; it is likely to remain in the nanosecond rather than picosecond range available using time domain FLIM. Strobe-FLIM therefore complements existing techniques in providing rapid lifetime imaging, implemented with minimal adaptation of a standard microscope, in a format that retains the sensitivity and pixel density of fluorescence intensity imaging. Analysis is based on the ratio of two image frames and so the method is inherently capable of providing video rate FLIM. The technique is ideally suited for applications requiring fast, robust image analysis such as the mapping, on sub-second timescales, of molecular interactions within live cells or rapid measurement in high throughput systems of lifetime-based switching assays with digital readout. Because the stroboscopic technique is detector independent its flexibility could also provide lifetime measurements across a broad range of fluorescence-based analysis systems such as endoscopy or flow cytometry.

4. Methods

4.1 Microscopy

All images were acquired in wide field using a standard Nikon fluorescence microscope with a 40x magnification objective. Detection was via a Hamamatsu Orca CCD camera using a 20 ms exposure time. A Fianium white light laser was used for excitation and was coupled into the microscope via the lamp housing. A 600 nm short pass filter and 480/40 nm bandpass dichroic mirror were used to spectrally filter the excitation beam whilst a 705/40 nm bandpass detection filter was used. For live cell lifetime imaging, the laser pulse frequency was initially set to 1 MHz and an image acquired after a 100 ms delay to allow the system to stabilise. The laser pulse frequency was then switched to 30 MHz and after a further 100 ms stabilisation a second image was acquired. There was no discernible photobleaching due to this stabilization delay in fact repeated imaging over a minute could be achieved whilst maintaining fluorescence intensity stability. Image matrices were stacked in memory to minimise CPU load of the controlling PC. Image processing involved the simple subtraction of a fixed background, and division of the 30 MHz matrix by the 1 MHz matrix (scaled by 30x to keep the number of pulses per acquisition for the two laser pulse frequencies the same).

4.2 Cell preparation

The human osteosarcoma cells, U-2 OS (ATCC HTB-96) were cultured under in McCoy's 5a medium supplemented with 10% foetal calf serum (FCS), 1mM glutamine, and antibiotics and incubated at 37^0 C in an atmosphere of 5% CO_2 in air. For imaging experiments, cells were grown at a density of $1x10^5$ cells ml^{-1} on top of a 24x24 No. 1.5 coverslip (RA Lamb) in a 6 well plate (BD Falcon™) to a confluency of 60-70%. Cells were loaded with commercially available targeted nanocrystals using the Qtracker® 705 Cell Labeling Kit (from Invitrogen; Catalog Number - Q25061MP) at 4 nM. The QD labelling solution was added to the cells and incubated for 1 hour at 37^o C before washing twice with full growth media. One set of Qtracker® 705 loaded cells coverslips was immediately fixed (1h pos-loaded cells) and another let to incubate for 24h. Cells were fixed with 4% paraformaldehyde in PBS for 30 min at 4^o C. Following fixation the coverslips were then mounted onto slides, directly with ProLong® Gold antifade reagent (P36930, Invitrogen) and in PBS, for this a square well of approx 150 µl volume was shaped with adhesive plastic tape on the slide, finally for both cases the coverslips were fixed in place using clear nail polish. Live samples were pre-prepared in silicone multi-well plates, and sealed with a glass slide and cover-slips and mounted individually on a temperature controlled stage (TCS).

#107281 - $15.00 USD Received 6 Feb 2009; revised 13 Mar 2009; accepted 15 Mar 2009; published 18 Mar 2009

Appendix

Analytical derivation of stroboscopic response:
The analysis proceeds by considering an ensemble of N_T systems with microstates 1 and 2 under excitation. The time dependent rate equations for such an ensemble are:

$$\frac{dN_2}{dt} = I_p\left(N_1 - N_2\right) - \frac{N_2}{\tau} \qquad [A1]$$

$$\frac{dN_1}{dt} = -I_p\left(N_1 - N_2\right) + \frac{N_2}{\tau} \qquad [A2]$$

where τ is the relaxation lifetime between upper state 2 and lower state 1 and I_p is the excitation rate per system. If we introduce n as the factional number of systems in the upper state; $n = N_2 / N_T$ we obtain an expression:

$$\frac{dn}{dt} = I_p\left(1 - 2n\right) - \frac{n}{\tau} \qquad [A3]$$

We consider the excitation to be a periodic impulse of duration T_p and period T. After an initial transient the ensemble will achieve a dynamic equilibrium and respond with a periodic output of fixed amplitude. Using the assumption of $T_p << \tau$ (i.e. an impulse excitation) the excitation of the ensemble becomes temporally separate from the relaxation and equation 3 can be solved by separately integrating the rate equation during the excitation pulse and during the ensuing relaxation.

i.e.
$$\int_{n_l}^{n_u} \frac{1}{\left(1 - 2n\right)} dn = \int_0^{T_p} I_p dt \qquad [A4]$$

and
$$\int_{n_u}^{n_l} -\frac{1}{n} dn = \int_0^{T} \frac{1}{\tau} dt \qquad [A5]$$

where n_l is the fraction of systems in the upper state immediately before the excitation pulse and n_u the fraction immediately after the pulse. Using the results of the integrals in equations A4 and A5 the change in n during a single cycle, $\Delta n = (n_u - n_l)$ can be found:

$$\Delta n = \tfrac{1}{2} \frac{\left(e^{2I_pT_p} - 1\right)}{\left(e^{I_pT_p} - e^{-\frac{T}{\tau}}\right)} \left\{1 - e^{-\frac{T}{\tau}}\right\} \qquad [A6]$$

Relation to measured parameters

To translate this analysis to experiment the parameters, Δn and I_pT_p have to be related to a measurable. The change in n is proportional to the integrated output signal per excitation period. A dc detector would therefore return a signal, S_{dc} per unit time which is proportional to the average value of Δn over one period. The term I_pT_p represents the total number of excitation events during a single impulse and is related to measurable physical quantities by:

#107281 - $15.00 USD Received 6 Feb 2009; revised 13 Mar 2009; accepted 15 Mar 2009; published 18 Mar 2009

$$I_p T_p = \eta_{ex} \frac{E_p}{E_q} \frac{\sigma}{A} \qquad [A7]$$

Where E_p/A is the excitation pulse energy per unit area, η_{ex} is the delivery efficiency of that energy to the ensemble, E_q is the energy of the excitation quanta and σ is the absorption cross-section of the 2-level system. The total fluorescence signal per pulse can therefore be represented by:

$$S_c = \kappa \frac{\left(e^{2\alpha P} - 1\right)}{\left(e^{2\alpha P} - e^{-\frac{\gamma}{f_{ex}}}\right)} \left\{1 - e^{-\frac{\gamma}{f_{ex}}}\right\} \qquad [A8]$$

where κ is a detection constant relating the measureable output to the number of relaxation events i.e. the energy released from the ensemble, α is an excitation constant linking the incident power to the excitation impulse function and the temporal dynamics of the excitation and fluorescence response are represented by a pulse frequency, f_{ex} and a relaxation rate, γ. Equation [A8] provides a means to determine γ from steady state measurements of the output signal.

Acknowledgments

This work was funded by the Engineering and Physical Sciences Research Council, U.K. under grant no. EP/E013104/1, 'Stroboscopic excitation fluorescence lifetime imaging' and the Research Councils U.K. on the Basic Technology programme under grant no. GR/S23483/01 'Optical Biochips'.

#107281 - $15.00 USD Received 6 Feb 2009; revised 13 Mar 2009; accepted 15 Mar 2009; published 18 Mar 2009